Journal of Environmental Chemical Engineering 11 (2023) 110936

Contents lists available at ScienceDirect

Journal of Environmental Chemical Engineering

journal homepage: www.elsevier.com/locate/jece

Metal-Al layered double hydroxides synthesized from aluminum slags as efficient CO_2 adsorbents at pre- and post-combustion temperature

L. Santamaría, S.A. Korili, A. Gil *

INAMAT2, Departamento de Ciencias, Edificio de los Acebos, Universidad Pública de Navarra, Campus de Arrosadía, E-31006 Pamplona, Spain

ARTICLE INFO

Editor: Dong-Yeun Koh

Keywords:
Aluminum industrial waste
CO_2 adsorption
Isosteric heat
Layered double hydroxides
Carbon capture and storage technology

ABSTRACT

Layered double hydroxides (LDH) have been proposed as the materials that offer the best performance in the moderate-temperature range, between 200 and 450 °C, for CO_2 adsorption, so the effect of some synthesis parameters and surface modification on their adsorption capacities is herein investigated. This work reports the use of M^{2+} (Co, Mg, Ni and Zn)/Al layered double hydroxides synthesized with a 3:1 molar ratio by the co-precipitation method and using aluminum extracted from saline slags as source of this metal as CO_2 adsorbents. The synthesis and use of Zn/TiAl is also reported considering several proportions of Al-Ti. Structural characterization and comparison of the series has been achieved using powder X-ray diffraction (PXRD), scanning electron microscopy (SEM), nitrogen physisorption at —196 °C and thermogravimetry measurements (TGA). The performance of calcined LDH as CO_2 adsorbents was evaluated in the 50 – 400 °C temperature range and 80 kPa and results show that Ni_6Al_2 and Mg_6Al_2 samples present a significant adsorption capacity at low temperature (0.382 and 0.292 $mmol_{CO2}/g$, respectively). At 400 °C only Mg_6Al_2 maintains its high adsorption capacity (0.275 $mmol_{CO2}/g$) compared to the other calcined LDH. Its adsorption capacity at moderate-temperature range was proven to be better than that of a commercial Mg_6Al_2 sample. In all materials the CO_2 adsorption capacity at 200–450 °C increased by incorporating potassium (K_2CO_3 and KOH as sources) up to 0.58 $mmol_{CO2}/g$ for Mg_6Al_2 +K_2CO_3. The addition of the amine TEPA in the low-temperature range worked for Co_6Al_2 and Mg_6Al_2 (increment > 40 %). In the case of Zn_6Al_2, the partial substitution of Al by Ti also increased the CO_2 adsorption capacity from 0.177 to 0.244 $mmol_{CO2}/g$, finding isosteric heats between 17.07 and 23.30 kJ/mol using the Clausius-Clapeyron equation.

1. Introduction

The measures implemented over the years to mitigate CO_2 emissions, such as the price of its emissions, are trying to decrease the concentration of CO_2 in the atmosphere. Diverse strategies have been proposed for Carbon Capture, Utilization and Storage (CCUS), aiming to avoid both non-biogenic and biogenic CO_2 emissions [1,2]. In the case of the Sorption Enhanced Water - Gas Shift (SEWGS) reaction, the primary fuel is first burned with the help of steam or oxygen, resulting in CO + H_2. The CO is then converted to CO_2 through a water gas shift reaction that requires moderate temperatures, between 200 and 450 °C, and high pressures, more than 10 bar. In this case, adsorbent materials have been proposed to retain the CO_2, in such a way that it also improves the conversion rate of the reaction. Another alternative would be to retain the CO_2 from the exhaust pipes, at lower temperatures and atmospheric pressure. These two options would correspond to those known as pre-combustion and post-combustion strategies, which can be related to general minimization and purification methods [3].

The adsorbent materials that can be used for pre-combustion capture must meet a series of conditions [3]: efficiency, selectivity towards CO_2 (other substances that are commonly present in these effluents are Hg, SO_2 or NOx), thermal and mechanical stability over several cycles, good sorption-desorption kinetics and positive response to the presence of steam. In the materials in which only physical interactions will participate, such as zeolites, activated carbons or aluminum oxide; or those materials with interactions of a chemical nature, such as calcium oxide or lithium zirconate; there is a requirement of either lower or higher temperatures, and they can also present drawbacks due to the presence of water [4,5]. Likewise, it has been cited that MOF-type materials can also suffer from a decline in their CO_2 adsorption capacity when in the presence of steam [6]. As alternative materials that show greater efficiency to retain CO_2 by combining physical and chemical adsorption and

* Corresponding author.
E-mail address: andoni@unavarra.es (A. Gil).

https://doi.org/10.1016/j.jece.2023.110936
Received 30 May 2023; Received in revised form 31 July 2023; Accepted 2 September 2023
Available online 3 September 2023

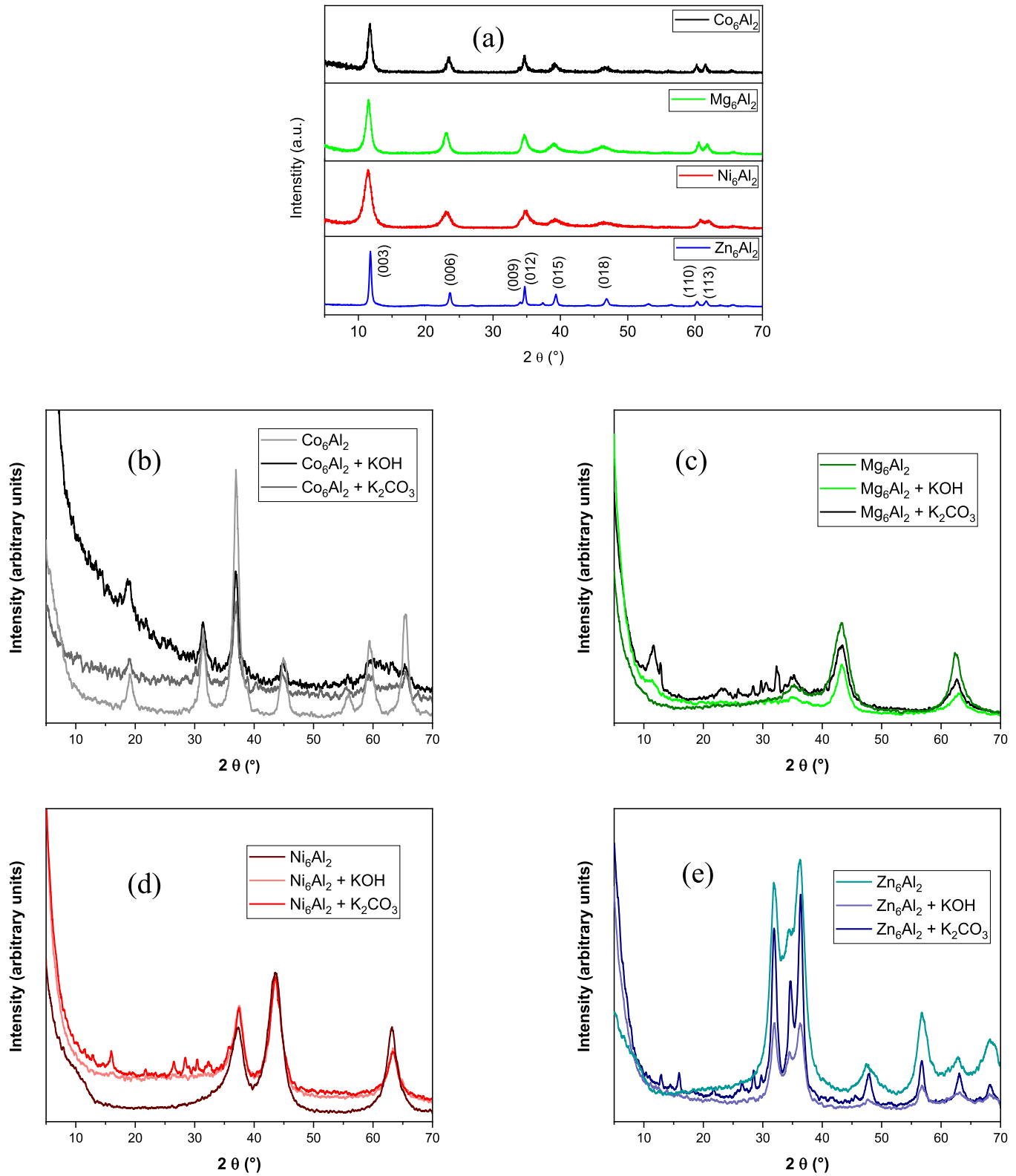

Fig. 1. Powder X-ray diffraction patterns of the non-calcined **(a)** and calcined samples (without modification and modified with KOH or K_2CO_3) with either cobalt **(b)**, magnesium **(c)**, nickel **(d)** and zinc **(e)** as M^{2+}.

also being resistant to the presence of water vapor, with relatively good thermal stability, arise Laminar Double Hydroxides (LDH).

LDH have been proposed as the materials that offer the best performance in the moderate temperature range for CO_2 adsorption. However, there is still room for improvement in terms of their adsorption capacity, mechanical stability in multicycle processes (adsorption-desorption) and adsorption kinetics. Thus, some strategies that are being developed for this technical upgrading can refer to the study of the LDH synthesis processes and internal structure (cations, M^{2+}/M^{3+} ratio, anions), to the synthesis of composite/hybrid adsorbent materials or to the alkalization

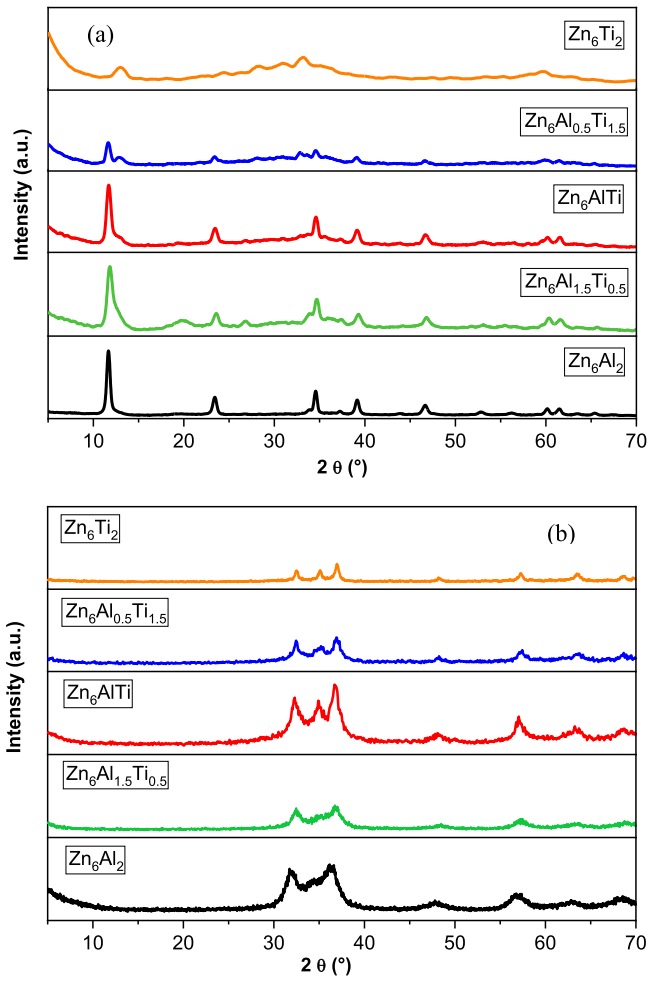

Fig. 2. Powder X-ray diffraction patterns of non-calcined **(a)** and calcined **(b)** $Zn_6Al_xTi_y$.

of the LDH surface by a simple impregnation procedure. Alternatively, it has also been proposed to modify the working conditions in terms of temperature, pressure or steam content.

When it comes to increasing the CO_2 adsorption capacity of LDH, impregnation with different amounts of K, and especially using K_2CO_3, is the most widely reported procedure [7–9]. Thus, Walspurger et al. [10] propose that the promotion of LDH with K_2CO_3 can encourage the carbonation of periclase (MgO). The formation of $MgCO_3$ can be catalyzed by a high enough concentration of a carbonate species such as K-CO_3-Al in equilibrium with CO_2. Another alternative mechanism is the one proposed by Hoffman and Pennline [11] and Yang and Kim [12]. In addition to potassium, other alkali metal or alkaline earth cations that have been used to improve the adsorbent properties of LDH are: Na [13–15], Cs [16–18] and Sr [16].

As the purpose of this study is to tackle a global environmental issue, the impact of the adsorbent synthesis process must not be neglected. Choosing environmental-safe materials with low costs is crucial for its potential upscaling. Taking a step further with the promotion of a circular economy model and a zero-waste goal is to be aimed for: selection of materials such as the use hazardous waste to extract the aluminum and prevent the material from ending up in secure deposits at best can be an interesting choice [19,20].

In the present work, the CO_2 adsorption capacity in a wide range of temperatures (between 50 and 400 °C) of various series of LDH prepared with Al^{3+} extracted from saline slags is reported. The effect of either the divalent cation or the incorporation of titanium in several proportions as trivalent cation in the adsorption capacity is evaluated, as well as the modification of the surface properties by the incorporation of K from two sources, K_2CO_3 and KOH. In addition, the samples modified with KOH have been functionalized with an amine tetraethylenepentamine (TEPA) to test the adsorbent capacity in post-combustion conditions (up to 100 °C).

2. Experimental procedure

2.1. Materials

The reagents employed for the synthesis of LDH were: $Co(NO_3)_2 \bullet 6H_2O$ (Panreac, ≥ 98 %), $Mg(NO_3)_2 \bullet 6H_2O$ (Sigma-Aldrich, ≥ 99.99 %), $Ni(NO_3)_2 \bullet 6H_2O$ (Panreac, ≥ 98 %), $TiCl_3$ (≥ 12 %, Sigma-Aldrich), $Zn(NO_3)_2 \bullet 6H_2O$ (Sigma-Aldrich, ≥ 98 %) and Na_2CO_3 (Sigma-Aldrich, ≥ 99.99 %). Nitric acid was used for pH adjustment together with sodium hydroxide (Panreac) which was also employed in the aluminum extraction process from the saline slags. Carbon dioxide (Praxair, 99.990 %), nitrogen (Praxair, 99.999 %) and helium (Praxair, 99.998 %) were used. Commercial hydrotalcite ($[(Mg_6Al_2(CO_3)(OH)_{16} \bullet 4H_2O]$, Sigma-Aldrich) was also used as reference. Ethanol (Panreac, max 0.02 % water) KOH (Scharlau, 90 %) K_2CO_3 (Sigma Aldrich) and tetraethylenepentamine (technical grade, Sigma-Aldrich) were use for the surface impregnation.

2.2. Hydrotalcite-like compounds synthesis and modifications

LDH had been synthesized with aluminum extracted from saline slags via a simple alkaline extraction process with NaOH [21]. The M^{2+}/M^{3+} chosen ratio was 3:1 using either cobalt, magnesium, nickel or zinc as M^{2+} and Al^{3+} from saline slags as M^{3+}. In the case of the Zn-Al LDH, another series was also synthesized in which Al^{3+} was partially substituted by Ti^{3+}, maintaining in all cases the Zn^{2+}/M^{3+} ratio equal to 3:1 [21]. In the synthesis method used, an aqueous solution of M^{2+} and the Al^{3+} extracted were dropwise added to an aqueous solution of Na_2CO_3 to a final volume of 400 mL, NaOH was used during the process to adjust the pH to 10. The mixture was stirred at 500 rpm and 60 °C for 60 min and aged for 24 h. The slurries obtained were centrifugated at 8000 rpm for 5 min and washed. This process was repeated several times until the washing water achieved a pH of 7. The samples were then dried at 80 °C for 16 h, manually grounded with a mortar and calcined at 400 °C for 4 h. The nomenclature used for the samples was M_6Al_2, for the cobalt, magnesium, nickel and zinc-based calcined LDH, and $Zn_6Al_xTi_y$ (with x + y = 2) for the calcined zinc LDH modified with titanium. Samples have been previously characterized and tested as drug adsorbents in aqueous media [21,22]. Therefore, this paper will highlight the most important results of the characterization obtained.

2.2.1. K_2CO_3 impregnation procedure

M_6Al_2 were impregnated with 15 wt% K_2CO_3 following the procedure used by Battha et al. [23], using an incipient wetness method [24]. In order to obtain 15 wt% K_2CO_3 loading, an aqueous solution (1.5 mL) containing 0.088 g of K_2CO_3 was added to 0.5 g of M_6Al_2 to the point of incipient wetness. The resulting paste was dried at 120 °C for 16 h and then calcined at 400 °C for 4 h. The amount of potassium was chosen following the results obtained by Wang et al. [25] after trying various percentages of K_2CO_3, ranging from 5 to 25 wt% and obtaining the best results at 15 wt%. The nomenclature used for the samples were M_6Al_2 +K_2CO_3.

2.2.2. KOH impregnation procedure

The four calcined samples were impregnated with the same amount of potassium than in the K_2CO_3 samples. The procedure followed was similar to that used by Thouchprasitchai et al. [26]. 1 g of calcined M_6Al_2 was dispersed in 0.1 mol/L KOH in ethanol and stirred at 120 rpm for 30 min. The samples were then washed with ethanol several times and finally dried for 10 h at 60 °C and atmospheric pressure. The

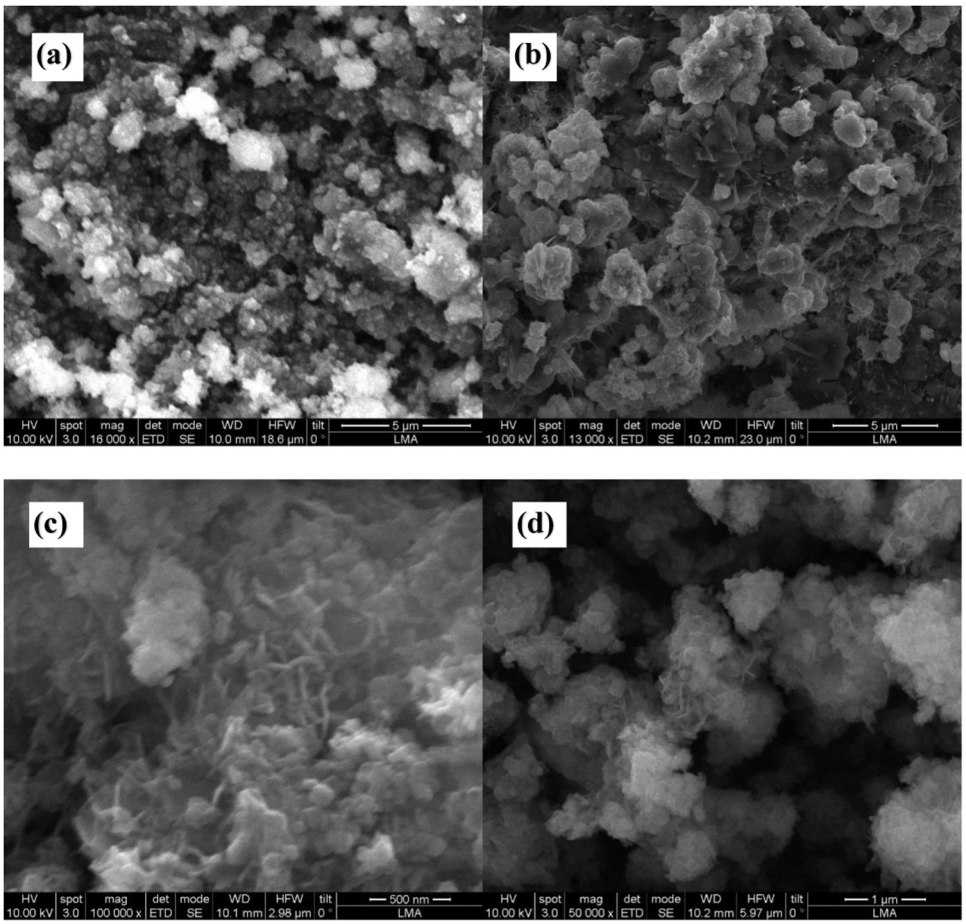

Fig. 3. SEM micrographs of the 4 Mg_6Al_2 samples synthesized: (a) Mg_6Al_2, (b) Mg_6Al_2+K_2CO_3, (c) Mg_6Al_2+KOH and (d) Mg_6Al_2+KOH+TEPA.

nomenclature used for the samples were M_6Al_2 +KOH.

2.2.3. TEPA impregnation procedure

Half the amount obtained previously (Section 2.2.2.) was separated and impregnated with TEPA at a 40/60 TEPA/M_6Al_2 +KOH proportion. The steps followed for obtaining the tetraethylenepentamine-functionalized samples were: first, a mixed solution of TEPA/ethanol at a constant mass to volume ratio of 1/2 was prepared and then was added to the M_6Al_2 + KOH samples and stirred for 30 min at 120 rpm. A slurry was obtained after a drying step of 1 h at 60 °C and the final adsorbent was collected after a 10 h drying process at 90 °C. The nomenclature used for the samples were M_6Al_2 +KOH+TEPA.

2.3. Characterization of the adsorbents

The crystalline phase of the samples was identified by powder X-ray diffraction (PXRD) using a Bruker D8 Advance Eco X-ray diffractometer with Ni-filtered Cu Kα radiation (λ = 0.1548 nm) at a scanning rate of 2° (2θ)/min. and a 2θ range from 5° to 70°.

The textural properties of the samples (0.4 g) were analyzed by nitrogen adsorption-desorption at − 196 °C using an accelerated surface area and porosimetry system (Micromeritics ASAP 2020 Plus adsorption analyzer). The samples were firstly degassed at 150 °C for 24 h under a pressure lower than 0.1 Pa. The Brunauer-Emmer-Teller (BET) method was applied to a relative pressure range of 0.05 – 0.20 in order to estimate the specific surface area (S_{BET}) of the samples. The external surface area (S_{ext}) and the micropore volumes ($V_{\mu p}$) were also estimated using the t-plot method.

Thermogravimetric measurements were performed on a Mettler Toledo TGA/DSC 3 + apparatus under an air atmosphere (50 cm^3/min) and using a 10 °C/min heating rate from room temperature up to 900 °C.

The chemical composition and morphological analysis of the samples was carried out by SEM (Inspect F50, accelerating voltage 10 Kv, BSED detector) and an EDAX detector obtained the X-ray Energy Dispersive Spectra (EDS).

2.4. CO_2 adsorption experiments

The adsorption of CO_2 was evaluated using a static volumetric method with a Micromeritics ASAP 2010 instrument and 0.2 g of solid. The samples were pre-treated at a heating rate of 10 °C/min, under a flow of He at 200 °C for 2 h, evacuated for 60 min and then the degassing continued while cooling down the sample until a pressure of less than 0.6 Pa was achieved at the adsorption temperature. CO_2 (Praxair, 99.990 %) adsorption data were collected in the pressure range between 6 and 80 kPa.

3. Results and discussion

3.1. Adsorbents characterization

The PXRD patterns of the fresh and calcined M_6Al_2 LDH and also impregnated M_6Al_2 +K_2CO_3 and M_6Al_2 +KOH are summarized in Fig. 1. Co_6Al_2 sample shows the crystal structure of the Co_3O_4 spinel with peaks at (showing 2θ and (*hkl*) reflections): 19° (111), 31° (220), 37° (311), 45° (400), 56° (422), 59° (511) and 65° (440). The impregnation of the sample with KOH or K_2CO_3 did not display any new peaks but the same peaks with less definition, peaks at 59° and 65° are less defined and blurred together in KOH sample. The Mg_6Al_2 sample presents the periclase crystal structure of MgO when calcined, the main peaks appeared

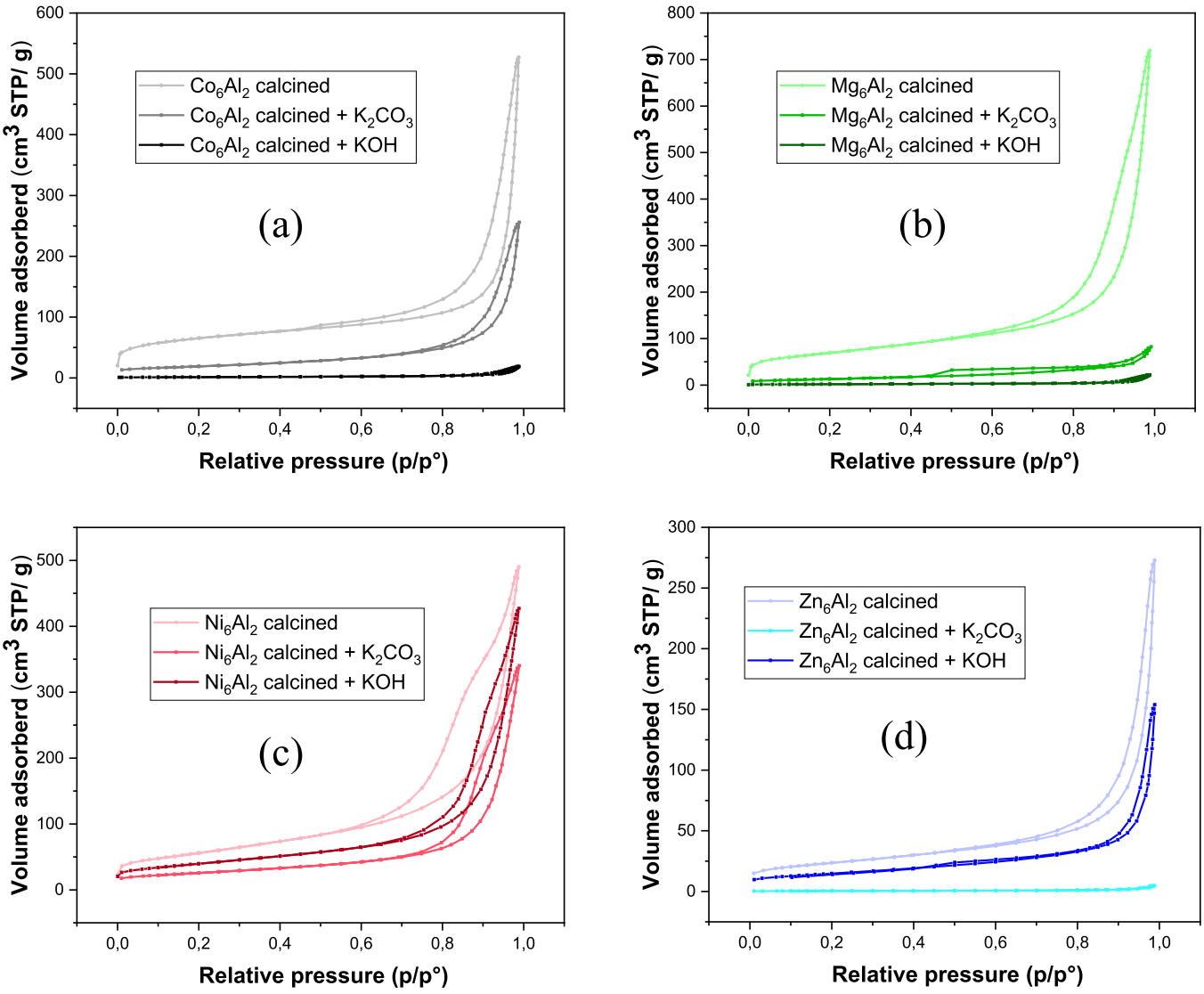

Fig. 4. The N_2 adsorption-desorption isotherms of the calcined samples (without modification and modified with KOH or K_2CO_3) with either cobalt (a), magnesium (b), nickel (c) and zinc (d) as M^{2+}.

at 35° (111), 43° (200) and 62° (220) planes. Samples impregnated with potassium show the periclase peaks together with a peak at 11°, revealing the rehydration of the structure (as is the main peak (003) of the LDH) and a series of small peaks between 25 and 35 2θ degrees in the carbonate sample, typical of K_2CO_3. In the Ni_6Al_2 sample nickel oxide (NiO) was formed with peaks at 37° (111), 43° (200) and 63° (220) and the Zn_6Al_2 sample was transformed into zincite (ZnO) when calcined (typical peaks at 32, 36 and 57 2θ degrees corresponding to (100), (101) and (110) planes, ref. pattern 00–005–0664). In both cases a different structure can be appreciated only in the carbonate impregnation, with a peak appearing at ~15° and a group of peaks at between 25° and 35° (Ref. pattern 00–016–0820).

The PXRD patterns of the non-calcined and calcined $Zn_6Al_xTi_y$ are summarized in Fig. 2. For the non-calcined samples, the crystallinity decreased with the increase of the titanium content and no diffraction reflections corresponding to titanium compounds were observed in the XRD patterns, suggesting that titanium was incorporated into the LDH structure or well dispersed into the LDH surface. The distinct basal (003) reflection, characteristic of LDH-like materials, was found around 11.7°. The small basal observed for Zn_6Ti_2 suggested that the LDH structure was not properly formed. After calcination at 400 °C, the structure was destroyed and zincite (ZnO) was found in all the cases. No diffraction reflections corresponding to TiO_2 phases, anatase or rutile, were observed suggesting a high dispersion or a low crystallinity of the oxides.

The modification of the adsorbents surface has been studied by means of SEM technology. As they will prove to have the best adsorption capacity (see 3.2), Mg_6Al_2 samples are shown in Fig. 3. The Mg_6Al_2 sample (**3a**) shows the typical LDH arrangement, with laminar plate-like structures. In Fig. 3b, corresponding to the Mg_6Al_2 +K_2CO_3 sample, another pattern can be found, showing sharp and straight structures. This salt appears throughout the sample and its presence will be translated into a bigger loss of surface (see next paragraph). The appearance of these kind of arrangements has been reported before [16,17,27]. Samples Mg_6Al_2 +KOH and Mg_6Al_2 +KOH+TEPA, corresponding to Fig. 3c and d respectively, show no difference with the original structure, no new structures are found. The data obtained by EDS shows that the average Mg/Al ratio in the surface of the sample is ~2.71. Sample M_6Al_2 +K_2CO_3 had a 14.87 wt% of potassium in its surface while sample Mg_6Al_2 +KOH had an average of 1.93 wt% of potassium, being that the reason why no new structures were found in this sample and its smaller decrease of surface.

The N_2 adsorption-desorption results of the LDH can be seen in Figs. 4 and 5. According to the IUPAC classification, all samples

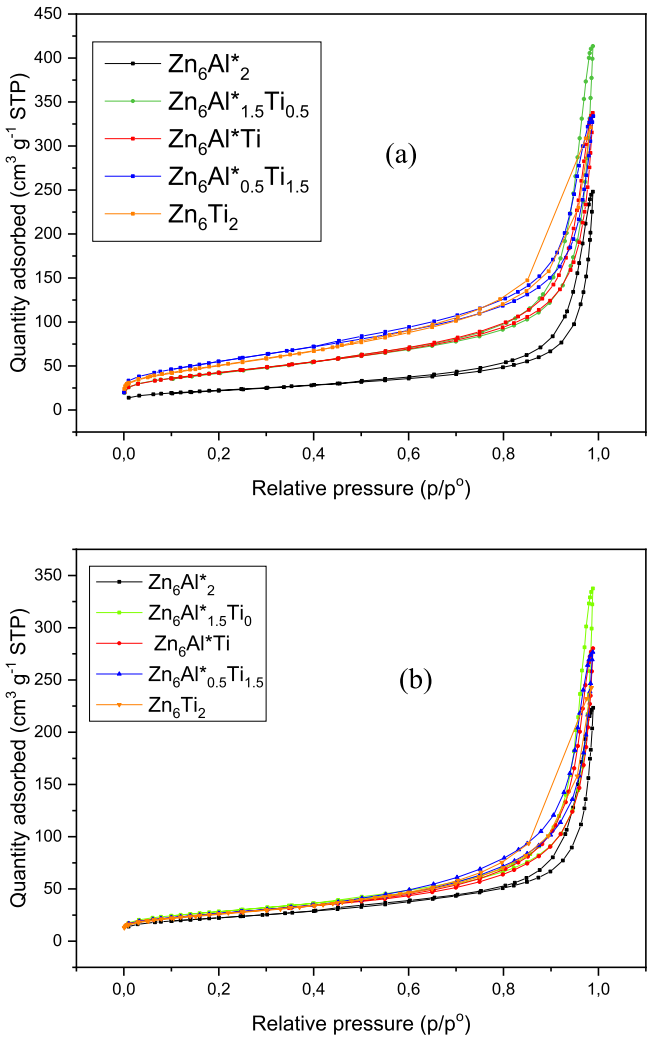

Fig. 5. The N_2 adsorption-desorption isotherms of non-calcined (a) and calcined (b) $Zn_6Al_xTi_y$.

Table 1
Textural properties of the M-Al LDH and M_6Al_2 modified with potassium samples.

Sample		S_{BET} (m^2/g)	S_{ext} (m^2/g)	$V_{\mu p}$ (cm^3/g)
Co_6Al_2	Non-calcined	141	137	0.0006
	Calcined	220	169	0.0273
	Calcined with KOH	107	95	0.0056
	Calcined with K_2CO_3	66	57	0.0046
Mg_6Al_2	Non-calcined	115	103	0.0053
	Calcined	245	218	0.0127
	Calcined with KOH	153	143	0.0046
	Calcined with K_2CO_3	47	46	0.0002
Ni_6Al_2	Non-calcined	113	103	0.0042
	Calcined	200	189	0.0042
	Calcined with KOH	141	131	0.0044
	Calcined with K_2CO_3	90	78	0.0056
Zn_6Al_2	Non-calcined	79	71	0.0037
	Calcined	83	73	0.0046
	Calcined with KOH	52	47	0.0022
	Calcined with K_2CO_3	34	30	0.0024

presented a type II adsorption isotherm, confirming the existence of nonporous or macroporous adsorbents. A hysteresis loop of the type H3 was identified in all the samples, usually found in laminar particles which show pores with a slit shape, that has no adsorption limit at high

Table 2
Textural properties of the Zn-Al/Ti LDH and $Zn_6Al_xTi_y$ samples.

Sample		S_{BET} (m^2/g)	S_{ext} (m^2/g)	$V_{\mu p}$ (cm^3/g)
Zn_6Al_2	Non-calcined	78	69	0.0045
	Calcined	83	73	0.0046
$Zn_6Al_{1.5}Ti_{0.5}$	Non-calcined	152	145	0.0027
	Calcined	100	91	0.0041
$Zn_6Al_1Ti_1$	Non-calcined	152	148	0.0013
	Calcined	93	86	0.0029
$Zn_6Al_{0.5}Ti_{1.5}$	Non-calcined	199	199	0
	Calcined	95	89	0.0023
Zn_6Ti_2	Non-calcined	184	184	0
	Calcined	95	95	0

relative pressures, thus indicating a weak reliability in the total pore volume and also the pore distribution [28]. BET specific surface area (S_{BET}), specific external surface area (S_{ext}) and specific micropore volume (Vμp) of the non-calcined, calcined and calcined and potassium-modified samples can be found in Table 1. In the case of M_6Al_2 sample series, TEPA-modified samples are not portrayed as the temperature needed during the degassing step (150 °C), that tries to get rid of the adsorbed water and gases, would imply the loss of TEPA as seen in the thermogravimetric tests. Calcined samples have S_{BET} superior to 200 except in the case of zinc were only 83 m^2/g were obtained. This could be related to the higher crystallinity of this sample, a common fact of this LDH [29–32], its better-ordered structure can imply a lesser amount of adsorption sites. Even though the BET surface results have been proven of not having a direct cause-effect on the CO_2 adsorption capacity [16,33], the fact that zinc sample has less than half the available surface could be related to its poorer results. KOH-impregnation of the samples brings a loss of surface between 30 % and 50 % and the impregnation with K_2CO_3 reduces it even more with results showing a decrease of surface between 55 % and 80 %. Adsorption results will show that this loss of surface does not imply a decrease in the CO_2 adsorption capacity, as CO_2 will be attracted to the alkaline properties that potassium brings. In the case of the $Zn_6Al_xTi_y$ series (see Table 2) the S_{BET} increased with the addition of titanium up to a maximum value of 199 m^2/g in the case of $Zn_6Al_{0.5}Ti_{1.5}$. The results of S_{ext} and Vμp confirm the non-porous character of the samples. When the samples were calcined, S_{BET} decreased in all cases, except in the case of Zn_6Al_2 where the S_{BET} slightly increases.

Thermal analysis of the M_6Al_2 +KOH+TEPA samples was performed in order to analyze the thermal stability of the samples impregnated with TEPA and thus select the maximum temperature of the CO_2 adsorption experiments of these samples. The decomposition behavior of TEPA on its own has been analyzed by Thouchprasitchai et al. [26] and showed a 97 % loss as TEPA decomposed between 120 and 260 °C preceded by a small 3 % water loss at lower temperature. Five mass loss steps were observed and the results were summarized in Table 3. The thermogravimetric analysis (upper lines) and differential thermal analysis (lower lines) results obtained for the four samples are displayed in Fig. 6. All the samples have a first step at around 100 °C, bigger in the case of cobalt and magnesium samples, which is assigned to the loss of loosely bound water and gases. From 250° to 450 °C the second major loss occurs which corresponds to the loss of TEPA. In some samples, like nickel, this loss is divided into two steps. Surface interactions of the impregnated TEPA onto M_6Al_2 +KOH samples have a delaying effect on the TEPA degradation of more than 100 °C. Magnesium sample has different behavior which can be seen in the 10 % loss at around 200 °C, attributed to the loss of interlaminar water and a second peak located at 400 °C that comes from dehydroxylation/decarbonation process together with the loss of TEPA. These peaks, located at the same position of the non-calcined MgAl-LDH [22], appear because of the memory effect of the LDH and the great affinity of this sample to atmospheric water vapor. Differences in the TEPA-impregnated and calcined samples show a ~30

Table 3
Mass losses (wt%) in the steps indicated from the thermogravimetric analyses of the M_6Al_2 +KOH+TEPA series.

Sample	1	2	3	4	5	TOTAL (wt%)
Co_6Al_2	0–150 °C	150–270 °C	270–450 °C	370–500 °C	500–900 °C	
	91.73	83.69	73.79	67.77	65.01	35.0
Mg_6Al_2	0–150 °C	150–270 °C	270–450 °C	370–500 °C	500–900 °C	
	92.64	79.75	67.43	55.20	52.31	47.7
Ni_6Al_2	0–150 °C	150–270 °C	270–450 °C	370–500 °C	500–900 °C	
	96.80	91.11	77.50	71.01	69.41	30.5
Zn_6Al_2	0–150 °C	150–270 °C	270–450 °C	370–500 °C	500–900 °C	
	95.85	88.44	75.34	67.62	65.88	34.1

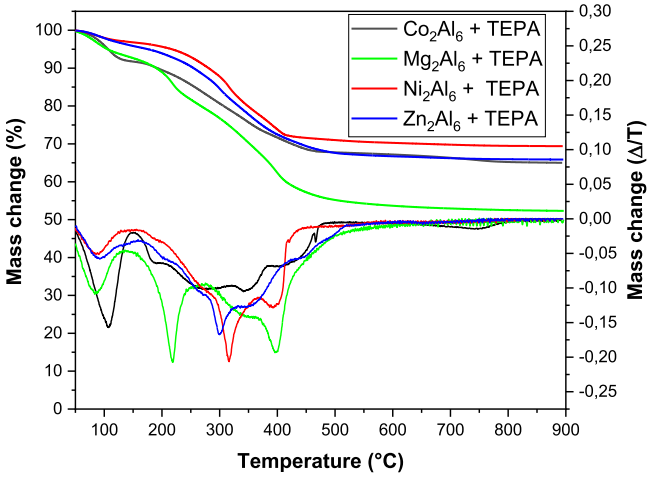

Fig. 6. TG and DTG curves of the calcined and modified with KOH + TEPA LDH.

% loss, assigned to TEPA disappearance.

3.2. CO_2 adsorption experiments

Several techniques such as thermogravimetric analysis (TGA), temperature-programmed desorption (TPD) or volumetric gas sorption can be used for testing the CO_2 adsorption capacity of a sample. For calcined LDH at moderate temperatures, TGA is the most commonly used [7,27,34–36] as is fast and inexpensive and can be used at pressures higher than 1 atm although its results are not as precise as using volumetric gas sorption equipment [37]. The volumetric method has been used in this study, and previously by a few others [38,39].

The CO_2 adsorption capacity was evaluated for the materials, previously treated at 200 °C, at several temperatures in the range of 50 and 400 °C. The experimental isotherms at these temperatures for $Zn_6Al_xTi_y$ are shown in Fig. 7. The maximum adsorption capacities for the solids at 50 °C and 80 kPa were between 0.177 and 0.244 $mmol_{CO2}/g$, for Zn_6Al_2 and Zn_6Ti_2 respectively. The behavior of the isotherms showed that the maximum amount adsorbed, as a function of the pressure gradient, decreased with an increase in temperature up to values of 0.073–0.081 $mmol_{CO2}/g$. It can also be observed that the incorporation of titanium caused an increase in the CO_2 adsorption capacity with respect to Zn_6Al_2. At 50 °C the amount adsorbed by Zn_6Ti_2 was 1.4 times higher than that of the starting solid. The shape presented by the isotherms shows that the amount of CO_2 adsorbed at low pressures was high and grew steadily with the increment in pressure. From these results, the strong interaction with the adsorption centers was confirmed. This interaction was mostly physical since it decreased with temperature.

The isosteric heat of adsorption allows us to describe the heat effects produced during the adsorption of a gas, in this case CO_2. Isosteric heat defines the energy change resulting from the phase change of an

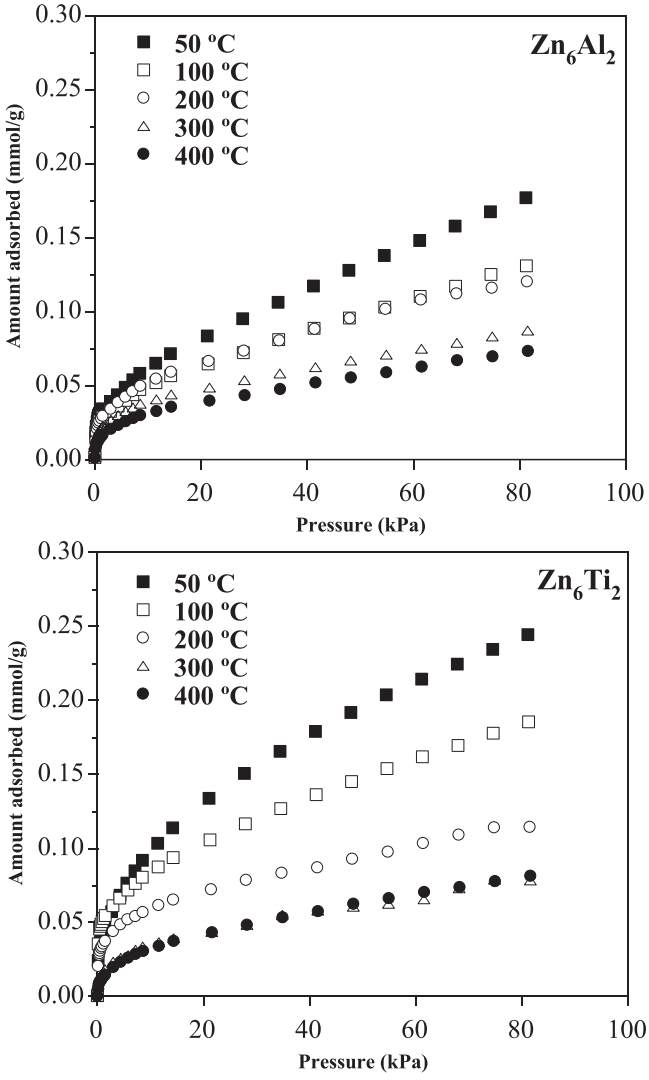

Fig. 7. CO_2 adsorption isotherm at 50, 100, 200, 300 and 400 °C for Zn_6Al_2 and Zn_6Ti_2.

infinitesimal number of molecules at constant pressure and temperature and a specific charge of adsorbate. The Clausius-Clapeyron equation allows us to calculate the isosteric heat of adsorption [40], which relates the isosteric heat to the change in pressure of the bulk gas phase as a consequence of a change in temperature for a constant amount of adsorbed gas. The equation can be written as:

$$q_{st} = -R\left[\frac{\partial lnp}{\partial(1/T)}\right]_n \quad (1)$$

where p (kPa) is the equilibrium pressure, n is the amount of gas

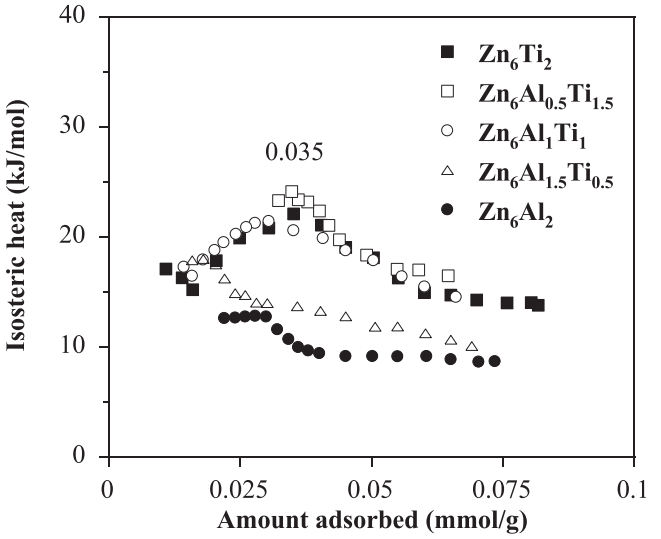

Fig. 8. Isosteric heat of CO_2 adsorption as a function of the amount of CO_2 adsorbed on the $Zn_6Al_xTi_y$ samples.

Table 4
Isosteric heats of adsorption at zero coverage.

Samples	q_{st}^0 (kJ/mol)[a]	q_{st}^0 (kJ/mol)[b]
Zn_6Al_2	4.02	12.62
$Zn_6Al_{1.5}Ti_{0.5}$	4.85	17.87
$Zn_6Al_1Ti_1$	11.27	17.25
$Zn_6Al_{0.5}Ti_{1.5}$	16.86	23.30
Zn_6Ti_2	7.38	17.07

[a] From the Henry constant.
[b] From the Clausius-Clapeyron equation.

adsorbed at temperature T (K) and R (kJ/mol·K) is the universal gas constant. The evolution of the isosteric heats of adsorption calculated from Eq. (1) versus the quantity adsorbed by each sample is presented in Fig. 8. It is possible to show that the isosteric heats of adsorption varied with the surface loading. A maximum is obtained at 0.035 $mmol_{CO2}/g$. This maximum has been related to the coating of the hydrotalcites surface with CO_2 [41,42]. Once the maximum is reached, the adsorption on lower energy sites of the surface and the formation of multilayers of CO_2 adsorbed may be the reasons for the steady decrease of the isosteric heat of adsorption with the increment of loading.

The limiting heat, q_{st}^0, can be determined from the temperature dependence of Henry's constant by applying the Clausius-Clapeyron equation in the low region [42,43]. It has been reported that the Henry's constant is an important characteristic of adsorption because it provides an indication of the strength of adsorption and the isosteric heat of adsorption at low pressure. There are various possibilities to calculate the Henry's constant (H), but it is possible to calculate it from the isotherm if there are sufficient data in the low-pressure region available [40]. In this case, the Eq. (1) can be also written as:

$$q_{st} = -R\left[\frac{\partial \ln H_i}{\partial(1/T)}\right]_n \quad (2)$$

The results found are also included in Table 4. The values found show that with the presence of Ti the values of the constant increase with respect to Zn_6Al_2, the highest values being those obtained for $Zn_6Al_{0.5}Ti_{1.5}$. The limiting heats obtained from Fig. 7 have been also included in Table 4. The values are higher than those obtained when calculating and from Henry's constant, but the trend is the same, also obtaining that the highest value corresponds to $Zn_6Al_{0.5}Ti_{1.5}$.

The CO_2 adsorption isotherms obtained at 50 and 400 °C of the

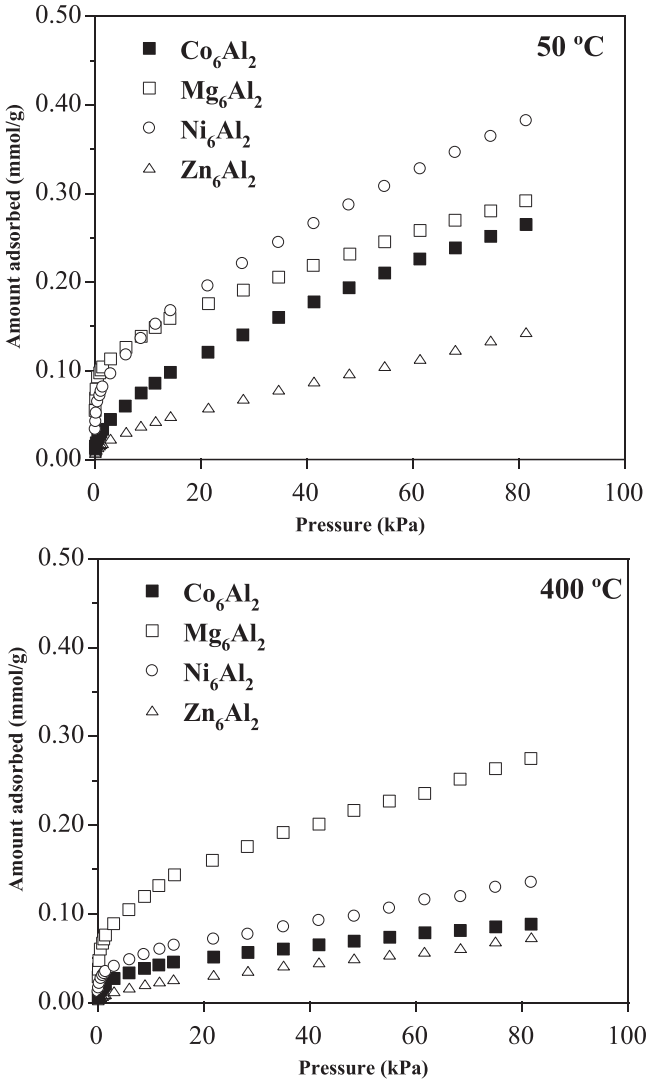

Fig. 9. Comparison of the CO_2 adsorption capacity of the different non-impregnated samples at 50 and 400 °C.

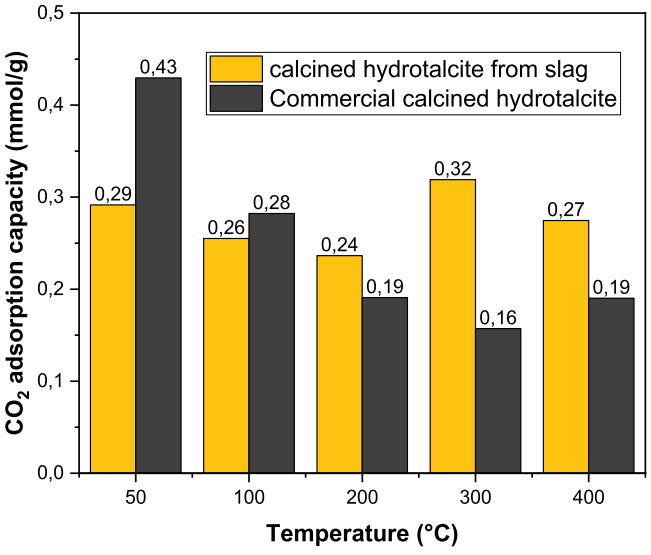

Fig. 10. CO_2 – adsorption capacity differences between a commercial sample Mg_6Al_2 and that synthesized from saline slags.

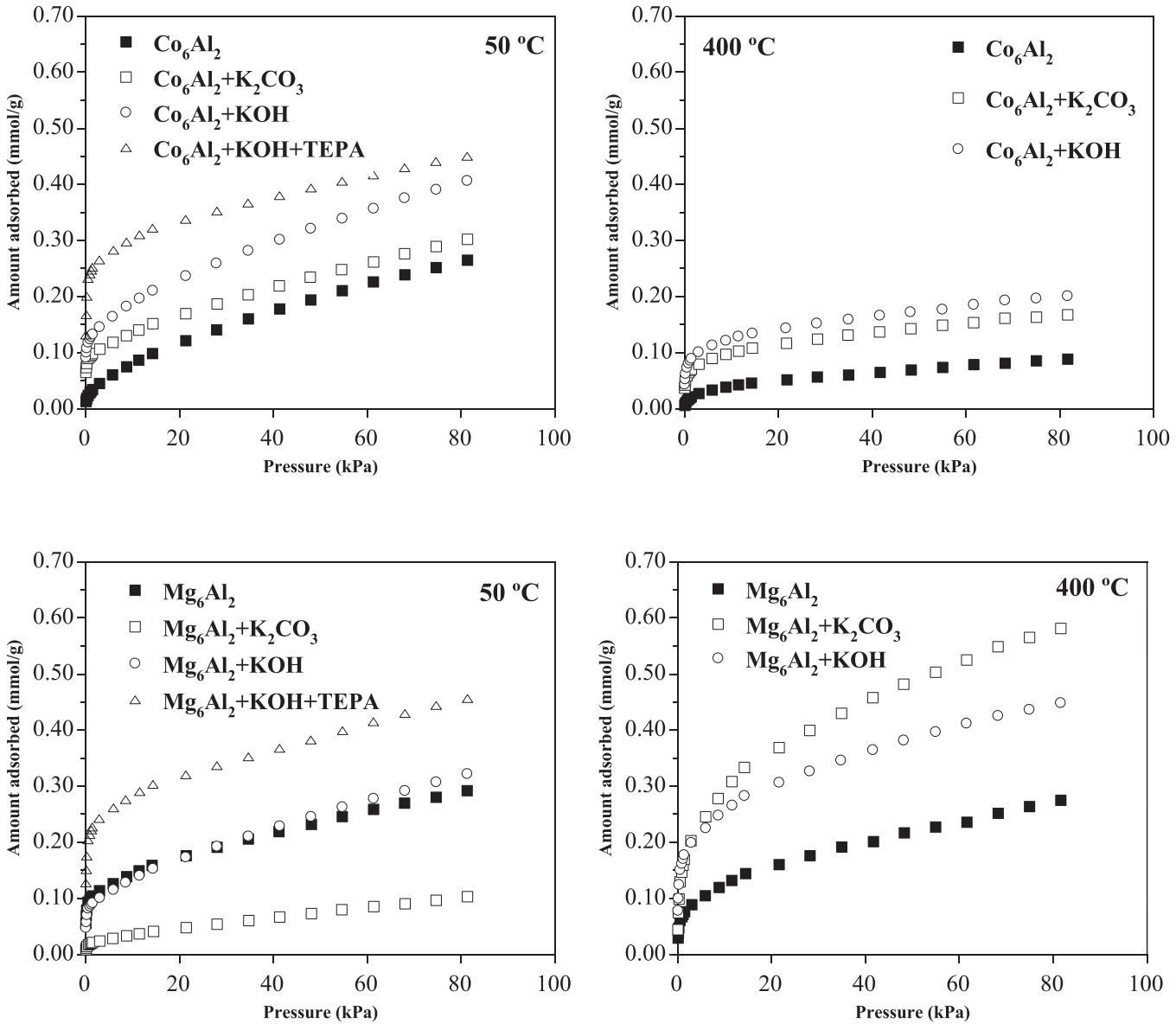

Fig. 11. Comparison of the CO_2 adsorption capacity of the impregnated Co_6Al_2 and Mg_6Al_2 at 50 and 400 °C.

calcined LDH with different M^{2+} (Co, Mg, Ni and Zn) are summarized in Fig. 9. At 50 °C the sample Ni_6Al_2 is the solid with the highest adsorption capacity, followed by Mg_6Al_2, Co_6Al_2 and Zn_6Al_2, which has the lowest capacity. Both Ni_6Al_2 and Mg_6Al_2 are characterized by their significant adsorption capacity at low pressures. This initial capacity is what allows them to remain above the other two samples in the rest of the pressure range. If the amounts of CO_2 adsorbed at 80 kPa are considered, we would have 0.382, 0.292, 0.265 and 0.144 $mmol_{CO2}/g$, respectively. There are a few studies that highlight the potential of Ni_6Al_2 as CO_2 adsorbent: Hanif et al. [14] obtained results with exfoliated Ni_6Al_2 similar to that of Mg_6Al_2, Sparks et al. [44] obtained synthesized Mg/Ni/Al samples with better adsorption capacity than MgAl on their own and Tsuji et al. [45] obtained the best results when using Ni instead of Mg, Co, Cu or Zn, although samples were not calcined beforehand. Ni_6Al_2 catalysts have been widely studied for the CO_2 methanation reaction as they are one of the most effective in the group VIIIB metals together with Ru and Rh catalysts [46], but also offer enviable low cost and ample availability compared to them [47]. Ni_6Al_2 offer a dual function: capture and conversion of CO_2 could be better achieved with these samples. When considering the moderate temperature range 200–400 °C, more adequate for pre-combustion application, Mg_6Al_2 offers the best results with a maximum adsorption capacity of 0.275 mmol/g. At 400 °C (see Fig. 9), it can be seen how Mg_6Al_2 maintains its adsorption capacity, while the other materials suffered a significant reduction in theirs. The maximum values found in these cases are 0.136 (Ni_6Al_2), 0.088 (Co_6Al_2) and 0.074 $mmol_{CO2}/g$ (Zn_6Al_2).

As Mg_6Al_2 sample provided the greatest outcome, this sample adsorption capacity was compared to that of a commercial hydrotalcite (also with a Mg/Al ratio of 3/1 and calcined at 400 °C for 4 h). The results at several temperatures and 80 kPa pressure are represented in Fig. 10. The commercial Mg_6Al_2 seems to reduce its capacity as the temperature increases and has the best result at 50 °C. The Mg_6Al_2 synthesized from slag has more potential in the range of pre-combustion-working temperature as its best capacity is obtained at 300 °C.

The adsorption results of the samples modified with potassium (either KOH or K_2CO_3) and TEPA are represented in Figs. 11 and 12. The experiments performed at 50 °C show that the best results are obtained by Co_6Al_2 and Mg_6Al_2, specially with the TEPA-functionalized samples (maxima adsorption capacity up to 80 kPa: 0.450 and 0.456 $mmol_{CO2}/$

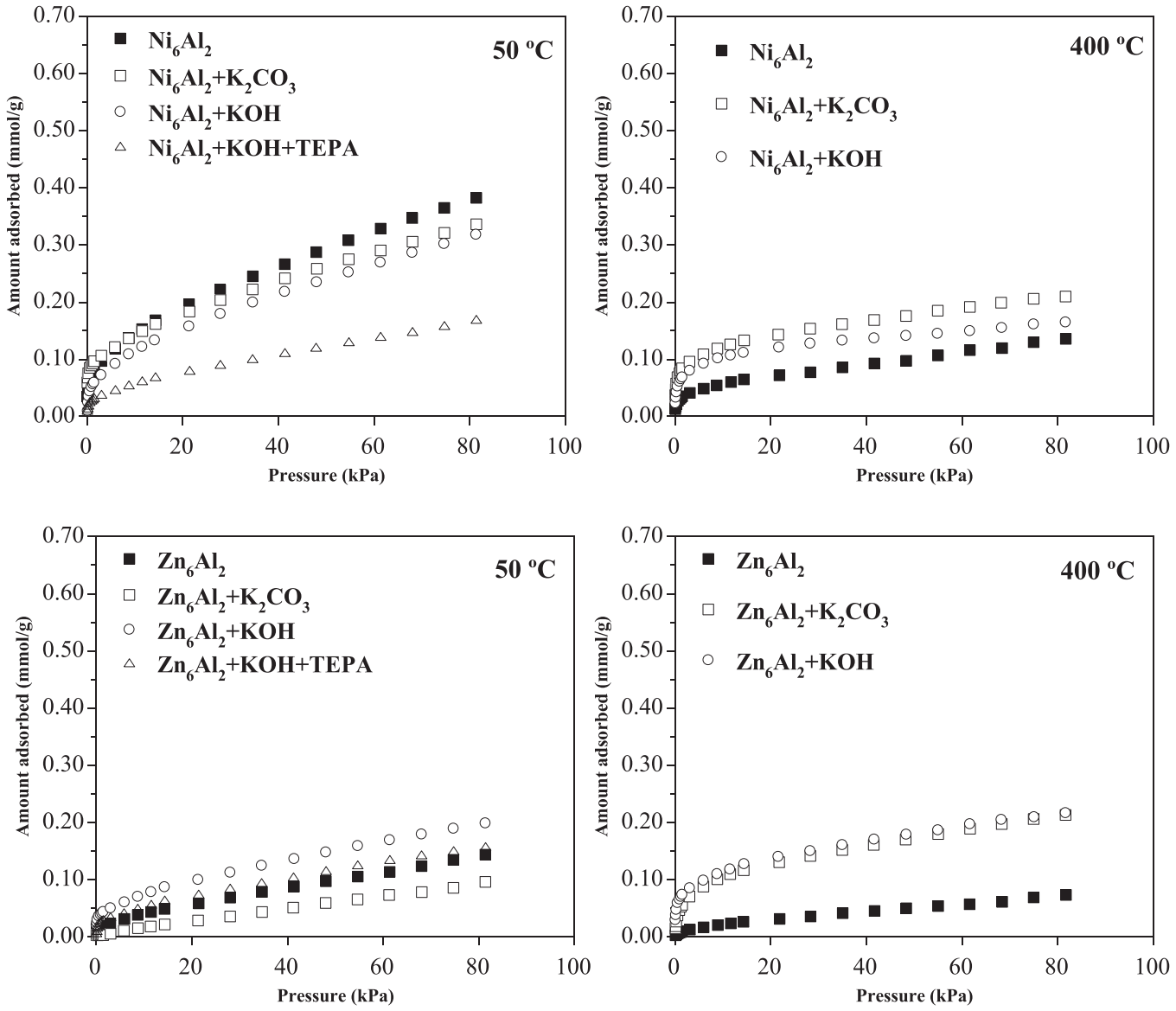

Fig. 12. Comparison of the CO_2 adsorption capacity of the impregnated Ni_6Al_2 and Zn_6Al_2 at 50 and 400 °C.

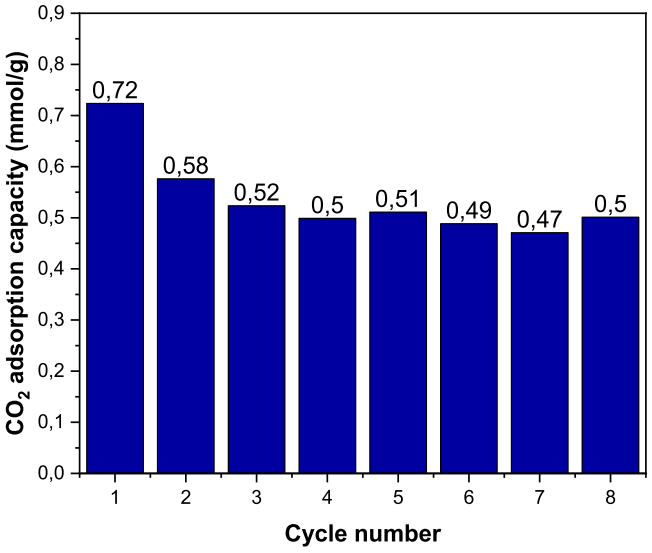

Fig. 13. CO_2 – adsorption capacity of K_2CO_3-modified MgAl LDH at 400 °C over a series of cycles.

g). This could be related to the presence of adsorbed water in these samples (seen in TGA analysis) as water vapor is known to ameliorate CO_2 adsorption capacity [48]. At this range of temperature KOH works better than K_2CO_3, in fact the latter reduces the adsorption capacity of the non-modified samples in three cases, as the alkalinity boost that provides K_2CO_3-impregnation does not seem to compensate the severe loss of available surface. At 400 °C Mg_6Al_2 gives the best results (Mg_6Al_2-K_2CO_3, 0.58 $mmol_{CO2}/g$). The incorporation of KOH and K_2CO_3 overall increase the adsorption capacity of the samples and present similar improvement in cobalt and zinc samples whereas in magnesium and nickel the impregnation with carbonate works better.

One of the most critical aspects to examine for industrial implementation is the durability of the adsorbents. As there is usually a lack of stability in the initial adsorption capacity of the M_6Al_2 and is not cost effective to change the adsorbent after each cycle, the working capacity of a sample is the most adequate feature to measure. Having the best results, K_2CO_3-impregnated Mg_6Al_2 adsorption capacity was put to the test in a series of adsorption-desorption cycles at 400 °C using the pressure swing approach, as is faster and more energy-efficient. Results obtained are presented in Fig. 13. The initial adsorption capacity in the first cycle (0.72 $mmol_{CO2}/g$) is reduced to 0.58 $mmol_{CO2}/g$ in the second

Table 5
Comparison of the CO_2 adsorption capacity of various LDH, potassium promoted or synthesized from slags.

	Composition	CO_2 uptake (mmol/g)	CO_2 uptake after K_2CO_3 impregnation	Adsorption conditions	Reference
LDH Synthesized from slags	MgFeAl-LDH from red mud and ferronickel slag	1.59		25 °C and 1 bar	[20]
	MgFeAl-LDH from commercial chemicals	1.45		25 °C and 1 bar	[20]
	$Ca_{1.89}Mg_{0.89}Al_{1.0}$-LDH from blast furnace slag	1.66		400 °C, 1 bar	[21]
	Mg_6Al_2 LDH from aluminum slag	0.27	0.58 (0.72)	400 °C, 0.8 bar	This work
Potassium-promoted LDH	commercial Mg_6Al_2 LDH	0.19		400 °C, 0.8 bar	This work
	Mg_3Al-CO_3	0.53	0.85	400 °C	[22]
	Mg_3Al-CO_3	0.22	0.83	400 °C, 1 atm	[23]
	Mg_4Al-CO_3	0.45	0.96	350 °C	[24]
	$Mg_{0.70}Al_{0.30}$-(CO_3)	0.06	0.37	400 °C, 1 bar	[25]

cycle and later stabilizes at around 0.50 $mmol_{CO2}/g$ for the next 6 cycles, which could be considered its working capacity. The initial drop is due to the fraction of adsorbate that is irreversibly chemisorbed and thus, cannot be easily removed. This remaining fraction is known to be pressure dependent [16] and also affected by the preparation method of the LDH [49]. As can be seen, the initial adsorption capacity, 0.72 $mmol_{CO2}/g$ is superior to that obtained in the series performed at different temperatures (Fig. 10) as the latter sample had been previously subjected to cycles at lower temperatures.

To our best knowledge, this is the first time that LDH synthesized from slags have been promoted with potassium or amines to test their CO_2 adsorption capacity. The results obtained were compared to those reported in literature from other LDH obtained from waste materials or promoted with K_2CO_3 (see Table 5). Results obtained are within the range of magnesium-aluminum LDH.

4. Summary and conclusions

This study gives an insight of the overall performance of calcined LDH synthesized from aluminum slags when subjected to several modification strategies (M^{2+}, M^{3+} and surface modification) in an attempt to boost its CO_2 adsorption capacity at both low and moderate temperatures. Calcined LDH with aluminum extracted from saline slags and a M^{2+}/M^{3+} ratio of 3:1 were tested as adsorbents over a range of temperatures for pre-combustion (200–450 °C) and post-combustion (< 100 °C) CO_2 capture. Cobalt, magnesium, nickel and zinc are tested as M^{2+}, with nickel-containing calcined LDH having the best adsorption capacity at lower temperatures followed by Mg_6Al_2. The latter maintains the adsorption capacity in the moderate-temperature range, performing better than the commercial sample at pre-combustion temperatures. The effect of aluminum substitution by titanium while maintaining the Zn^+/M^{3+} ratio caused an increment in the adsorption capacity (1.4 times higher) at low temperatures although this difference decreased with temperature increase. Surface modification with KOH or K_2CO_3 give various effects; while KOH improves usually the adsorption capacity of the samples, K_2CO_3 impregnation tends to work better at higher temperatures, giving the best overall result on the Mg_6Al_2 sample (0.58 $mmol_{CO2}/g$). This sample, M_6Al_2 +K_2CO_3 was tested in a series of adsorption-desorption cycles at 400 °C using the pressure swing approach and its working capacity was found to be 0.50 $mmol_{CO2}/g$. M_6Al_2 +KOH samples were impregnated with the amine TEPA in with the aim of improving their performance at post-combustion conditions, obtaining good results for cobalt and magnesium samples.

CRediT authorship contribution statement

L. Santamaría: Conceptualization, Methodology, Writing – original draft, Investigation, Writing – review & editing. **S.A. Korili:** Supervision, Writing – review & editing. **A. Gil:** Conceptualization, Methodology, Writing – original draft, Supervision, Writing – review & editing.

Declaration of Competing Interest

The authors declare that they have no known competing financial interests or personal relationships that could have appeared to influence the work reported in this paper.

Data Availability

No data was used for the research described in the article.

Acknowledgements

The authors are grateful for financial support from the Spanish Ministry of Science and Innovation (MCIN/AEI/10.13039/501100011033) through project PID2020-112656RB-C21. LS thanks the Universidad Pública de Navarra for a post-doctoral Margarita Salas grant, financed by the European Union-Next Generation EU.

References

[1] E.I. Koytsoumpa, C. Bergins, E. Kakaras, The CO_2 economy: Review of CO_2 capture and reuse technologies, J. Supercrit. Fluids 132 (2018) 3–16, https://doi.org/10.1016/j.supflu.2017.07.029.
[2] M.N. Anwar, A. Fayyaz, N.F. Sohail, M.F. Kholchar, M. Baqar, W.D. Khan, K. Rasool, M. Rehan, A.S. Nizami, CO_2 capture and storage: a way forward for sustainable environment, J. Environ. Manag 226 (2018) 131–144, https://doi.org/10.1016/j.jenvman.2018.08.009.
[3] L. Santamaría, S.A. Korili, A. Gil, Layered double hydroxides for CO_2 adsorption at moderate temperatures: synthesis and amelioration strategies, Chem. Eng. J. 455 (2023), 140551, https://doi.org/10.1016/j.cej.2022.140551.
[4] H. Th, J. Reijers, S.E.A. Valster-Schiermeier, P.D. Cobden, R.W. Van Den Brink, Hydrotalcite as CO_2 sorbent for sorption-enhanced steam reforming of methane, Ind. Eng. Chem. Res. 45 (2006) 2522–2530, https://doi.org/10.1021/ie050563p.
[5] J.M. Silva, M.A. Soria, L.M. Madeira, Challenges and strategies for optimization of glycerol steam reforming process, Renev. Sustain. Energy Rev. 42 (2015) 1187–1213, https://doi.org/10.1016/j.rser.2014.10.084.
[6] A.M. Fracaroli, H. Furukawa, M. Suzuki, M. Dodd, S. Okajima, F. Gándara, J. A. Reimer, O.M. Yaghi, Metal–organic frameworks with precisely designed interior for carbon dioxide capture in the presence of water, J. Am. Chem. Soc. 136 (2014) 8863–8866, https://doi.org/10.1021/ja503296c.
[7] X. Zhu, C. Chen, Q. Wang, Y. Shi, D. O'Hare, N. Cai, Roles for K_2CO_3 doping on elevated temperature CO_2 adsorption of potassium promoted layered double oxides, Chem. Eng. J. 366 (2019) 181–191, https://doi.org/10.1016/j.cej.2019.01.192.
[8] S. Li, Y. Shi, Y. Yang, Y. Zheng, N. Cai, High-performance CO_2 adsorbent from interlayer potassium-promoted stearate-pillared hydrotalcite precursors, Energy Fuels 27 (2013) 5352–5358, https://doi.org/10.1021/ef400914r.
[9] X. Zhu, C. Chen, Y. Shi, D. O'Hare, N. Cai, Aqueous miscible organic-layered double hydroxides with improved CO_2 adsorption capacity, Adsorption 26 (2020) 1127–1135, https://doi.org/10.1007/s10450-020-00209-4.
[10] S. Walspurger, P.D. Cobden, O.V. Safonova, Y. Wu, E.J. Anthony, High CO_2 storage capacity in alkali-promoted hydrotalcite-based material: In situ detection of reversible formation of magnesium carbonate, Chem. A Eur. J. 16 (2010) 12694–12700, https://doi.org/10.1002/chem.201000687.
[11] J.S. Hoffman, H.W. Pennline, Study of regenerable sorbents for CO2 capture, in: 17th Annu. Int. Pitts Burgh Coal Conf., 2000.
[12] J.H. Yang, J.H. Kim, Hydrotalcites for adsorption of CO_2 at high temperature, Korean J. Chem. Eng. 23 (2006) 77–80, https://doi.org/10.1007/BF02705695.
[13] S. Kim, S.G. Jeon, K.B. Lee, High-Temperature CO_2 sorption on hydrotalcite having a high Mg/Al molar ratio, ACS Appl. Mater. Interfaces 8 (2016) 5763–5767, https://doi.org/10.1021/acsami.5b12598.

[14] A. Hanif, M. Sun, S. Shang, Y. Tian, A.C.K. Yip, Y.S. Ok, I.K.M. Yu, D.C.W. Tsang, Q. Gu, J. Shang, Exfoliated Ni-Al LDH 2D nanosheets for intermediate temperature CO_2 capture, J. Hazard. Mater. 374 (2019) 365–371, https://doi.org/10.1016/j.jhazmat.2019.04.049.

[15] Y.J. Min, S.M. Hong, S.H. Kim, S.G. Jeon, High-temperature CO_2 sorption on Na_2CO_3-impregnated layered double hydroxides, Korean J. Chem. Eng. 31 (2014) 1668–1673, https://doi.org/0.1007/s11814-014-0116-1.

[16] C.V. Miguel, R. Trujillano, V. Rives, M.A. Vicente, A.F.P. Ferreira, A.E. Rodrigues, A. Mendes, L.M. Madeira, High temperature CO_2 sorption with gallium-substituted and promoted hydrotalcites, Sep. Purif. Rechn. 127 (2014) 202–211, https://doi.org/10.1016/j.seppur.2014.03.007.

[17] E.L.G. Oliveira, C.A. Grande, A.E. Rodrigues, CO_2 sorption on hydrotalcite and alkali-modified (K and Cs) hydrotalcites at high temperatures, Sep. Purif. Technol. 62 (2008) 137–147, https://doi.org/10.1016/j.seppur.2008.01.011.

[18] A.C. Faria, R. Trujillano, V. Rives, C.V. Miguel, A.E. Rodrigues, L.M. Madeira, Alkali metal (Na, Cs and K) promoted hydrotalcites for high temperature CO_2 capture from flue gas in cyclic adsorption processes, Chem. Eng. J. 427 (2022), 131502, https://doi.org/10.1016/j.cej.2021.131502.

[19] A. Gil, S.A. Korili, Management and valorization of aluminum saline slags: current status and future trends, Chem. Eng. J. 289 (2016) 74–84, https://doi.org/10.1016/j.cej.2015.12.069.

[20] L. Santamaría, S.A. Korili, A. Gil, Layered double hydroxides from slags: Closing the loop. J. Environ. Chem. Eng., 2922, 10. https://doi.org/10.1016/j.jece.2021.106948.

[21] L. Santamaría, M. López-Aizpún, M. García-Padial, M.A. Vicente, S.A. Korili, A. Gil, Zn-Ti-Al layered double hydroxides synthesized from aluminum saline slag wastes as efficient drug adsorbents, Appl. Clay Sci. 187 (2020), 105486, https://doi.org/10.1016/j.clay.2020.105486.

[22] L. Santamaría, F. Devred, E.M. Gaigneaux, M.A. Vicente, S.A. Korili, A. Gil, Effect of the surface properties of Me^{2+}/Al layered double hydroxides synthesized from aluminum saline slag wastes on the adsorption removal of drugs, Microporous Mesoporous Mater. 309 (2020), 110560, https://doi.org/10.1016/j.micromeso.2020.110560.

[23] L.K.G. Bhatta, S. Subramanyam, M.D. Chengala, U.M. Bhatta, K. Venkatesh, Enhancement in CO_2 adsorption on hydrotalcite-based material by novel carbon support combined with K_2CO_3 impregnation, Ind. Eng. Chem. Res. 54 (2015) 10876–10884, https://doi.org/10.1021/acs.iecr.5b02020.

[24] J. Nataraj, S.Carvill, B.Hufton, J.Mayorga, S.Gaffney, T.Brzozowski, Materials Selectively Adsorbing CO_2 from CO_2 Containing Streams, EP Patent 1006079A1, 2000.

[25] J. Wang, X. Mei, L. Huang, Q. Zheng, Y. Qiao, K. Zang, S. Mao, R. Yang, Z. Zhang, Y. Gao, Z. Guo, Z. Huang, Q. Wang, Synthesis of layered double hydroxides/graphene oxide nanocomposite as a novel high-temperature CO_2 adsorbent, J. Energy Chem. 24 (2015) 127–137, https://doi.org/10.1016/S2095-4956(15)60293-5.

[26] N. Thouchprasitchai, N. Pintuyothin, S. Pongstabodee, Optimization of CO_2 adsorption capacity and cyclical adsorption/desorption on tetraethylenepentamine-supported surface-modified hydrotalcite, J. Environ. Sci. 65 (2018) 293–305, https://doi.org/10.1016/j.jes.2017.02.015.

[27] J.M. Silva, R. Trujillano, V. Rives, M.A. Soria, L.M. Madeira, High temperature CO_2 sorption over modified hydrotalcites, Chem. Eng. J. 325 (2017) 25–34, https://doi.org/10.1016/j.cej.2017.05.032.

[28] M. Thommes, Physical adsorption characterization of nanoporous materials, Chem. -Ing. -Tech. 82 (2010) 1059–1073, https://doi.org/10.1002/cite.201000064.

[29] S. Naseem, B. Gevers, R. Boldt, F.J.W.J. Labuschagné, A. Leuteritz, Comparison of transition metal (Fe, Co, Ni, Cu, and Zn) containing tri-metal layered double hydroxides (LDHs) prepared by urea hydrolysis, RSC Adv. 9 (2019) 3030–3040, https://doi.org/10.1039/c8ra10165e.

[30] C.A. Johnson, F.P. Glasser, Hydrotalcite-like minerals ($M_2Al(OH\ 6(CO_3)_{0.5}XH_2O$, where M = Mg, Zn, Co, Ni) in the environment: synthesis, characterization and thermodynamic stability, Clays Clay Min. 51 (2003) 1–8, https://doi.org/10.1346/CCMN.2003.510101.

[31] F.Z. Mahjoubi, A. Khalidi, M. Abdennouri, N. Barka, M-Al-SO_4 layered double hydroxides (M=Zn, Mg or Ni): synthesis, characterization and textile dyes removal efficiency, Desalin. Water Treat. 57 (2016) 21564–21576, https://doi.org/10.1080/19443994.2015.1124055.

[32] R. Manivannan, A. Pandurangan, Formation of ethyl benzene and styrene by side chain methylation of toluene over calcined LDHs, Appl. Clay Sci. 44 (2009) 137–143, https://doi.org/10.1016/j.clay.2008.12.017.

[33] Y. Yang, K. Chen, L. Huang, M. Li, T. Zhang, M. Zhong, P. Ning, J. Wang, S. Wen, Research on Li0.3Na0.18K0.52NO3 promoted Mg20Al-CO3 LDH/GO composites for CO2 capture, J. Ind. Eng. Chem. 102, 2021, pp. 86–94. ⟨https://doi.org/10.1016/j.jiec.2021.06.036⟩.

[34] K. Coenen, F. Gallucci, P. Cobden, E. van Dijk, E. Hensen, M. van Sint Annaland, Chemisorption working capacity and kinetics of CO2 and H2O of hydrotalcite-based adsorbents for sorption-enhanced water-gas-shift applications, Chem. Eng. J. 293, 2016, pp. 9–23. ⟨https://doi.org/10.1016/j.cej.2016.02.050⟩.

[35] R. Singh, M.K. Ram Reddy, S. Wilson, K. Joshi, J.C. Diniz da Costa, P. Webley, High temperature materials for CO_2 capture, Energy Procedia 1 (2009) 623–630, https://doi.org/10.1016/j.egypro.2009.01.082.

[36] L. Sun, Y. Yang, H. Ni, D. Liu, Z. Sun, P. Li, J. Yu, Enhancement of CO_2 adsorption performance on hydrotalcites impregnated with alkali metal nitrate salts and carbonate salts, Ind. Eng. Chem. Res. 59 (2020) 6043–6052, https://doi.org/10.1021/acs.iecr.9b05700.

[37] H.A. Patel, J. Byun, C.T. Yavuz, Carbon dioxide capture adsorbents: Chemistry and methods, ChemSusChem 10 (2017) 1303–1317, https://doi.org/10.1002/cssc.201601545.

[38] M.J. Ramírez-Moreno, I.C. Romero-Ibarra, M.A. Hernández-Pérez, H. Pfeiffer, CO_2 adsorption at elevated pressure and temperature on Mg-Al layered double hydroxide, Ind. Eng. Chem. Res. 53 (2014) 8087–8094, https://doi.org/10.1021/ie5010515.

[39] S.I. Garcés-Polo, J. Villarroel-Rocha, K. Sapag, S.A. Korili, A. Gil, Adsorption of CO_2 on mixed oxides derived from hydrotalcites at several temperatures and high pressures, Chem. Eng. J. 332 (2018) 24–32, https://doi.org/10.1016/j.cej.2017.09.056.

[40] S. Garcés-Polo, J. Villarroel-Rocha, K. Sapag, S.A. Korili, A. Gil, Comparative study of the adsorption equilibrium of CO_2 on microporous comercial materials at low pressures, Ind. Eng. Chem. Res. 52 (2013) 6785–6793, https://doi.org/10.1021/ie400380w.

[41] C. Nguyen, D.D. Do, Adsorption of supercritical gases in porous media: determination of micropore size distribution, J. Phys. Chem. B 103 (1999) 6900–6908, https://doi.org/10.1021/jp9906536.

[42] A. Gil, E. Arrieta, M.A. Vicente, S.A. Korili, Synthesis and CO_2 adsorption properties of hydrotalcite-like compounds prepared from aluminum saline slag wastes, Chem. Eng. J. 334 (2018) 1341–1350, https://doi.org/10.1016/j.cej.2017.11.100.

[43] S. Sircar, Estimation of isoteric heats of adsorption of single gas and multicomponent gas mixtures, Ind. Eng. Chem. Res. 31 (1992) 1813–1819, https://doi.org/10.1021/ie00007a030.

[44] D.E. Sparks, T. Morgan, P.M. Patterson, S.A. Tackett, E. Morris, M. Crocker, New sulfur adsorbents derived from layered double hydroxides. I: synthesis and COS adsorption, Appl. Catal. B Environ. 82 (2008) 190–198, https://doi.org/10.1016/j.apcatb.2008.01.012.

[45] M. Tsuji, G. Mao, T. Yoshida, Y. Tamaura, Hydrotalcites with an extended Al^{3+}-substitution: synthesis, simultaneous TG-DTA-MS study, and their CO_2 adsorption behaviors, J. Mater. Res 8 (1993) 1137–1142, https://doi.org/10.1557/JMR.1993.1137.

[46] S. Abate, K. Barbera, E. Giglio, F. Deorsola, S. Bensaid, S. Perathoner, R. Pirone, G. Centi, Synthesis, characterization, and activity pattern of Ni-Al hydrotalcite catalysts in CO_2 methanation, Ind. Eng. Chem. Res. 55 (2016) 8299–8308, https://doi.org/10.1021/acs.iecr.6b01581.

[47] S. Kawi, Y. Kathiraser, J. Ni, U. Oemar, Z. Li, E.T. Saw, Progress in synthesis of highly active and stable nickel-based catalysts for carbon dioxide reforming of methane, ChemSusChem 8 (2015) 3556–3575, https://doi.org/10.1002/cssc.201500390.

[48] N.E.H. Hadj-Abdelkader, A.P. Beltrao-Nunes, F. Belkhadem, N. Benselka, R. Roy, A. Azzouz, New insights in MgAl and MgFe-LDH affinity towards carbon dioxide – role of the hydrophilic character on CO_2 retention strength, Appl. Clay Sci. 198 (2020), 105829, https://doi.org/10.1016/j.clay.2020.105829.

[49] M.H. Halabi, M.H.J.M. De Croon, J. Van Der Schaaf, P.D. Cobden, J.C. Schouten, High capacity potassium-promoted hydrotalcite for CO_2 capture in H_2 production, Int. J. Hydrogen Energy 37 (2012) 4516–4525, https://doi.org/10.1016/j.ijhydene.2011.12.003.